PERGAMON

International Journal of Solids and Structures 37 (2000) 4455–4472

INTERNATIONAL JOURNAL OF SOLIDS and STRUCTURES

www.elsevier.com/locate/ijsolstr

# Interface forces in composite steel–concrete structure

Evangelos J. Sapountzakis*, John T. Katsikadelis

*Institute of Structural Analysis, Department of Civil Engineering, National Technical University of Athens, Zografou Campus, GR-157 73, Athens, Greece*

Received 26 February 1999; in revised form 5 May 1999

**Abstract**

In this paper a solution to the bending problem of reinforced concrete slabs stiffened by steel beams including creep and shrinkage effect is presented. The adopted model takes into account the resulting in-plane forces and deformations of the plate as well as the axial forces and deformations of the beam, due to combined response of the system. The analysis consists in isolating the beams from the plate by sections parallel to the lower outer surface of the plate. The forces at the interface, which produce lateral deflection and in-plane deformation to the plate, lateral deflection and axial deformation to the beam, are established using continuity conditions at the interface. The creep and shrinkage effect relative with the time of the casting and the time of the loading of the plate is taken into account. The solution of the arising plate and beam problems which are non-linearly coupled, is achieved using the Analog Equation Method (AEM). The adopted model, compared with those ignoring the in-plane forces and deformations, approaches the actual response of the plate–beams system more reliably. Moreover, it permits the evaluation of the shear forces at the interfaces, the knowledge of which is very important in the design of composite steel–concrete structures. The resulting deflections are considerably smaller than those obtained by other models. 

*Keywords:* Elastic stiffened plate; Reinforced plate with beams; Bending; Ribbed plate; Creep; Shrinkage; Composite steel–concrete structure

## 1. Introduction

The interest in composite reinforced concrete slabs stiffened by steel beams has been widespread in recent years due to the economic and structural advantages of such systems. Composite steel–concrete structures are efficient, economical and functional, while construction using steel beams as stiffeners of

* Corresponding author. Tel.: +30-1-772-1718; fax: +30-1-772-1820.
*E-mail address:* cvsapoun@central.ntua.gr (E.J. Sapountzakis).

0020-7683/00/$ - see front matter 
PII: S0020-7683(99)00156-0

concrete plates is a quick, familiar and economical method for long bridge decks or for long span slabs. The extensive use of the aforementioned plate structures necessitates a rigorous analysis.

In the extensive literature on static analysis of slab-and-beam structures, their behaviour was initially approximated by converting this system to an equivalent homogeneous slab of constant thickness using the stiffness properties of the beams and applying the orthotropic plate theory (Pama and Cusens, 1967; Powell and Ogden, 1969). This approximation may only be applicable when the stiffened plate satisfies two limitations. The first one is that ratios of spacing between two consecutive stiffeners to slab boundary dimensions are small enough to ensure approximate homogeneity of stiffness. The second limitation is that the ratio of stiffener rigidity to the slab rigidity must not become so large that the beam action is predominant.

Subsequently, in more refined approximations the adopted models for the analysis of the plate–beams system isolated the beams from the plate and neglected the shear forces at the interfaces (Cheung et al., 1994; Hu and Hartley, 1994; King and Zienkienwicz, 1968; Kukreti and Cheraghi, 1993; Kukreti and Rajapaksa 1990; Ng et al., 1990; de Paiva, 1996; Tanaka and Bercin, 1997). This assumption results in discrepancies from the actual response of the stiffened plate. Moreover, it does not allow the establishment of these forces, which are necessary for the design of composite or prefabricated structures.

In this paper the analysis of reinforced concrete slabs stiffened by steel beams including creep and shrinkage effect is presented. The adopted structural model is that employed by Sapountzakis and Katsikadelis (1998), which, contrary to the models used previously, takes into account the resulting in-plane forces and deformations of the plate as well as the axial forces and deformations of the beam, due to combined response of the system. Using this model, the study of the behaviour of a stiffened plate subjected to a lateral load and to the effects of creep and shrinkage is attempted. The analysis consists in isolating the beams from the plate by sections parallel to the lower outer surface of the plate. The forces at the interface producing lateral deflection and in-plane deformation to the plate, lateral deflection and axial deformation to the beam, are established using continuity conditions at the interface. The arising plate and beam problems, which are non-linearly coupled, are solved using the Analog Equation Method (AEM) (Katsikadelis, 1994; Nerantzaki, 1994). The adopted model describes better the actual response of the plate–beams system and permits the evaluation of the shear forces at the interface, the knowledge of which is very important in the design of the aforementioned structures (estimation of shear connectors). The evaluated lateral deflections of the plate–beams system are found to exhibit considerable discrepancy from those of other models, which neglect in-plane and axial forces and deformations. Finally, the opposed action of creep and shrinkage effect to the behaviour of the stiffened plate is investigated.

## 2. Statement of the problem

Consider a thin reinforced concrete plate having constant thickness $h_p$, occupying the domain $\Omega$ of the $x, y$ plane and stiffened by a set of parallel steel beams. The plate may have $J$ holes and is supported on its boundary $\Gamma = \cup_{j=0}^{J} \Gamma_j$, which may be piecewise smooth (Fig. 1), while the beams may have point supports. For the sake of convenience the $x$-axis is taken parallel to the beams. Let the time of the casting of the plate $t_{pc}$ be the beginning of the time considered $t$ and $t_{pl}$ be the time at which the plate is initially subjected to the lateral load $g = g(\mathbf{x})$, $\mathbf{x}$: $\{x, y\}$.

The solution of the problem at hand is approached by isolating the beams from the plate by sections in the lower outer surface of the plate and taking into account the tractions at the fictitious interfaces (Fig. 2). These tractions result in the loading of the beam as well as the additional loading of the plate. Their distribution is unknown and can be established by imposing

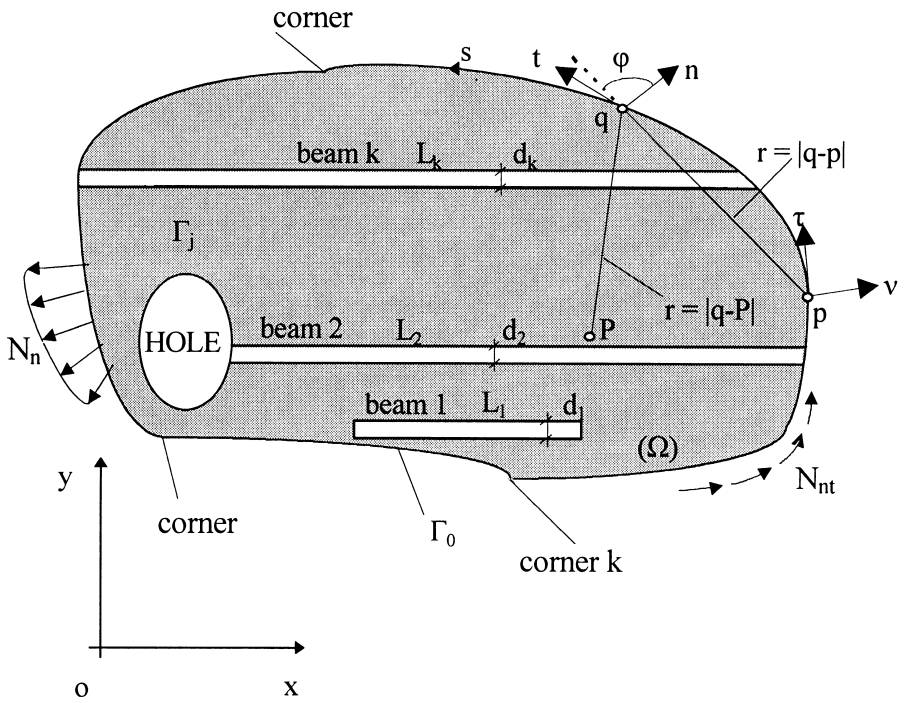


Fig. 1. Two-dimensional region $\Omega$ occupied by the plate.

displacement continuity conditions at the interfaces and using the procedure developed in this investigation.

The integration of the tractions along the width of the beam result in line forces per unit length which are denoted by $q_x$, $q_y$ and $q_z$. Taking into account that the torsional stiffness of the beam is small, the traction component $q_y$, in the direction normal to the beam axis, may be ignored. However, in a more refined model the influence of this component may also be considered. The other two components $q_x$ and $q_z$ produce the following loading along the trace of each beam.

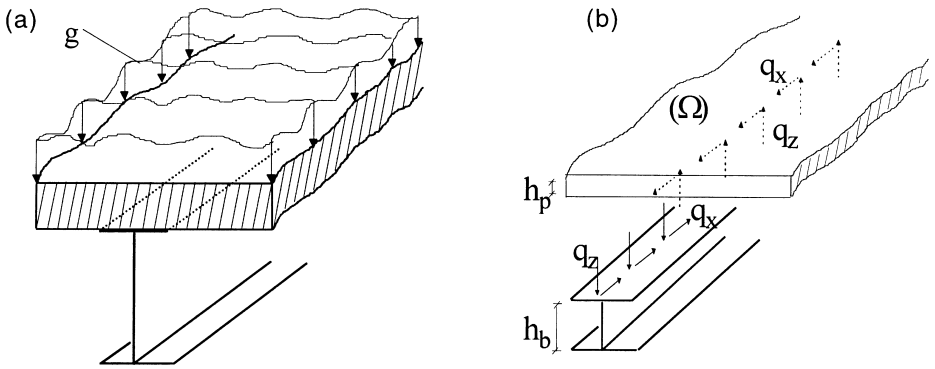


Fig. 2. Thin elastic plate stiffened by beams (a) and isolation of the beams from the plate (b).

### 2.1. In the plate

1. A lateral line load $-q_z$ at the interface.
2. A lateral line load $-\partial M_{\mathrm{p}}/\partial x$ due to the eccentricity of the component $q_x$ from the middle surface of the plate. $M_{\mathrm{p}}=q_x h_{\mathrm{p}}/2$ is the bending moment.
3. An in-plane line body force $q_x$ at the middle surface of the plate.

### 2.2. In each beam

1. A transverse load $q_z$.
2. A transverse load $\partial M_{\mathrm{b}}/\partial x$ due to the eccentricity of $q_x$ from the neutral axis of the beam cross section.
3. An in-plane axial force $q_x$.

The structural models of the plate and the beams are shown in Fig. 3.

On the basis of the above considerations the response of the plate and of the beams may be described by the following boundary value problems.

### 2.3. For the plate

The plate undergoes transverse deflection and in-plane deformation. Thus, for the transverse deflection we have

$$D\nabla^4 w_{\mathrm{p}} - \left(N_x\frac{\partial^2 w_{\mathrm{p}}}{\partial x^2} + 2N_{xy}\frac{\partial^2 w_{\mathrm{p}}}{\partial x\,\partial y} + N_y\frac{\partial^2 w}{\partial y^2}\right) = g - \sum_{k=1}^{K}\left(q_z^{(k)} + \frac{\partial M_{\mathrm{p}}^{(k)}}{\partial x}\right)\delta(y-y_k) \quad \text{in } \Omega \tag{1}$$

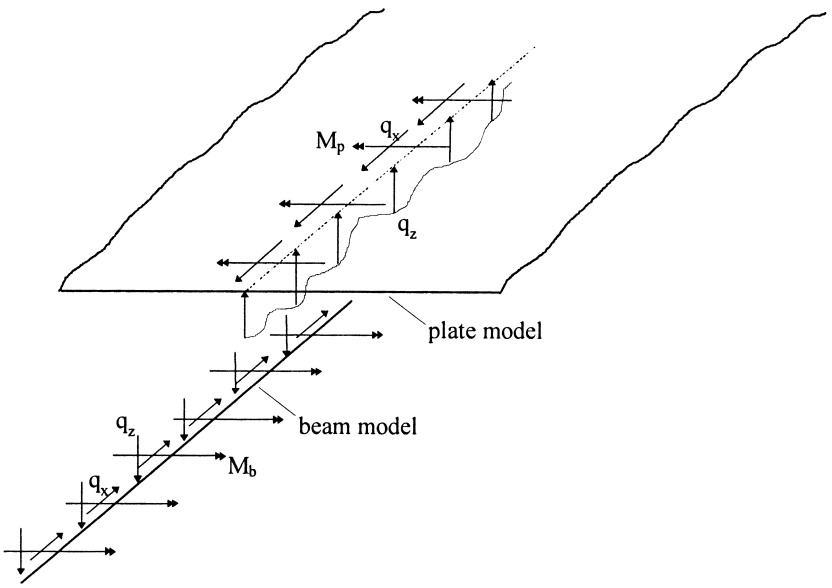


Fig. 3. Structural model of the plate and the beams.

$$\alpha_1 w_p + \alpha_2 V_n = \alpha_3 \tag{2a}$$

$$\beta_1 \frac{\partial w_p}{\partial n} + \beta_2 M_n = \beta_3 \quad \text{on } \Gamma \tag{2b}$$

$$\gamma_{1k} w_p + \gamma_{2k} \| T_n \|_k = \gamma_{3k} \quad \text{at the corner point } k \tag{2c}$$

where $w_p = w_p(\mathbf{x}, t)$ is the time dependent transverse deflection of the plate; $D(t) = E_p(t) h_p^3/12(1-\nu^2)$ is its time dependent flexural rigidity with $E_p$ being the elastic modulus and $\nu$ the Poisson ratio; $N_x = N_x(\mathbf{x}, t)$, $N_y = N_y(\mathbf{x}, t)$, $N_{xy} = N_{xy}(\mathbf{x}, t)$ are the membrane forces per unit length of the plate cross section at time $t$; $\delta(y-y_k)$ is the Dirac's delta function in the $y$-direction; $M_n$ and $V_n$ are the bending moment normal to the boundary and the effective reaction along it, respectively, and they are given as

$$M_n = -D\left( \frac{\partial^2 w_p}{\partial n^2} + \nu \frac{\partial^2 w_p}{\partial t^2} \right) \tag{3a}$$

$$V_n = -D\left[ \frac{\partial}{\partial n} \nabla^2 w_p - (\nu - 1) \frac{\partial}{\partial s} \frac{\partial^2 w_p}{\partial n \, \partial t} \right] \tag{3b}$$

$T_n$ is the twisting moment along the boundary given as

$$T_n = D(1-\nu)\left( \frac{\partial^2 w_p}{\partial s \, \partial n} - \kappa \frac{\partial w_p}{\partial s} \right) \tag{4}$$

and $\| T_n \|_k$ is its jump of discontinuity at the corner point $k$.

Finally, $a_i$, $\beta_i$, $\gamma_i$ ($i = 1, 2, 3$) are functions specified on the boundary $\Gamma$.

The boundary conditions (2a,b) are the most general linear boundary conditions for the plate problem also including the elastic support. It is apparent that all types of the conventional boundary conditions (clamped, simply supported, free or guided edge) can be derived from these equations by specifying appropriately the functions $a_i$ and $\beta_i$ (e.g. for a clamped edge it is $a_1 = \beta_1 = 1$, $a_2 = a_3 = \beta_2 = \beta_3 = 0$).

If the stresses are kept within the limits corresponding to the normal service conditions, assuming linear relationship between creep and the stress causing the creep and denoting by $t_p = t_{pl} - t_{pc}$, Trost's theory (Trost and Wolff, 1970) gives the tangent modulus of elasticity as

$$E_p(t) = \frac{E_{pl}}{1 + \chi \varphi(t, t_p)} \tag{5}$$

where $E_{pl}$ is the tangent modulus of elasticity of the plate at time $t_p$; $\chi$ is an ageing coefficient depending on strain development with time; $\varphi(t, t_p)$ is the creep coefficient related to the elastic deformation at $t_p$ days which is defined as (Eurocode, 1991)

$$\varphi(t, t_p) = \phi_{RH} \beta(f_{cm}) \beta(t_p) \beta_{cp}(t - t_p) \tag{6}$$

where $\varphi_{RH}$, $\beta(f_{cm})$ and $\beta(t_p)$ are factors depending on the relative humidity, the concrete strength and the concrete age at loading, respectively, which are defined as

$$\varphi_{RH} = 1 + (1 - RH/100)/(0.10^3 \sqrt{h_0}) \tag{7a}$$

$$\beta(f_{cm}) = 16.8/\sqrt{f_{cm}} \tag{7b}$$

$$\beta(t_{\mathrm{p}}) = 1/(0.1 + t_{\mathrm{p}}^{0.20}) \tag{7c}$$

where $RH$ is the relative humidity of the ambient environment in %; $h_0 = 2A_{\mathrm{p}}/u_{\mathrm{p}}$ is the notional size of the plate in mm; $A_{\mathrm{p}}$ is the area of the plate cross section; $u_{\mathrm{p}}$ is the plate perimeter in contact with the atmosphere; $f_{\mathrm{cm}}$ is the mean compressive strength of concrete in N/mm$^2$ at the age of 28 days. Moreover, $\beta_{\mathrm{cp}}(t-t_{\mathrm{p}})$ in Eq. (6) is a coefficient for the development of creep with time, which is estimated from

$$\beta_{\mathrm{cp}}(t - t_{\mathrm{p}}) = [(t - t_{\mathrm{p}})/(\beta_{\mathrm{H}} + t - t_{\mathrm{p}})]^{0.3} \tag{8}$$

where $\beta_{\mathrm{H}}$ is a coefficient depending on the relative humidity $RH$, given as

$$\beta_{\mathrm{H}} = 1.5[1 + (0.012RH)^{18}]h_0 + 250 \leq 1500 \tag{9}$$

Since the linear plate bending theory is considered, the components of the membrane force $N_x$, $N_y$, $N_{xy}$ do not depend on the deflection $w_{\mathrm{p}}$. They are given as

$$N_x = C\left(\frac{\partial u_{\mathrm{p}}}{\partial x} + \nu\frac{\partial v_{\mathrm{p}}}{\partial y}\right) \tag{10a}$$

$$N_y = C\left(\nu\frac{\partial u_{\mathrm{p}}}{\partial x} + \frac{\partial v_{\mathrm{p}}}{\partial y}\right) \tag{10b}$$

$$N_{xy} = C\frac{1-\nu}{2}\left(\frac{\partial u_{\mathrm{p}}}{\partial y} + \frac{\partial v_{\mathrm{p}}}{\partial x}\right) \tag{10c}$$

where $C(t) = E_{\mathrm{p}}(t)/(1-\nu^2)$; $u_{\mathrm{p}} = u_{\mathrm{p}}(\mathbf{x}, t)$ and $v_{\mathrm{p}} = v_{\mathrm{p}}(\mathbf{x}, t)$ are the displacement components of the middle surface of the plate arisen from the line body force $q_x$, the temperature distribution $T_{\mathrm{p}}(\mathbf{x}, t)$ due to the plate shrinkage and the possible boundary in-plane loading. These displacement components are established by solving independently the plane stress problem, which is described by the following boundary value problem (Navier's equations of equilibrium)

$$\nabla^2 u_{\mathrm{p}} + \frac{1+\nu}{1-\nu}\frac{\partial}{\partial x}\left[\frac{\partial u_{\mathrm{p}}}{\partial x} + \frac{\partial v_{\mathrm{p}}}{\partial y}\right] + \frac{1}{G_{\mathrm{p}}}q_x\delta(y - y_k) - 2\alpha\frac{1+\nu}{1-\nu}\frac{\partial T_{\mathrm{p}}}{\partial x} = 0 \quad \text{in } \Omega \tag{11a}$$

$$\nabla^2 v_{\mathrm{p}} + \frac{1+\nu}{1-\nu}\frac{\partial}{\partial y}\left[\frac{\partial u_{\mathrm{p}}}{\partial x} + \frac{\partial v_{\mathrm{p}}}{\partial y}\right] - 2\alpha\frac{1+\nu}{1-\nu}\frac{\partial T_{\mathrm{p}}}{\partial y} = 0 \tag{11b}$$

$$\gamma_1 u_{\mathrm{n}} + \gamma_2 N_{\mathrm{n}} = \gamma_3 \tag{12a}$$

$$\delta_1 u_{\mathrm{t}} + \delta_2 N_{\mathrm{t}} = \delta_3 \quad \text{on } \Gamma \tag{12b}$$

in which $G_{\mathrm{p}}(t) = E_{\mathrm{p}}(t)/2(1+\nu)$ is the shear modulus of the plate; $\alpha$ is the linear coefficient of thermal expansion; $N_{\mathrm{n}}$, $N_{\mathrm{t}}$ and $u_{\mathrm{n}}$, $u_{\mathrm{t}}$ are the boundary membrane forces and displacements in the normal and tangential directions to the boundary, respectively; $\gamma_i$, $\delta_i$ ($i$ = 1, 2, 3) are functions specified on $\Gamma$.

Assuming that creep and shrinkage are independent, the temperature distribution $T_{\mathrm{p}}(\mathbf{x}, t)$ is given as (Eurocode, 1991)

$$T_{\mathrm{p}}(\mathbf{x}, t) = \epsilon_{\mathrm{sp}}(t - t_{\mathrm{pc}})/\alpha \tag{13}$$

where $\epsilon_{\mathrm{sp}}(t-t_{\mathrm{pc}})$ is the shrinkage strain calculated from

$$\epsilon_{\mathrm{sp}}(t - t_{\mathrm{pc}}) = \epsilon_{\mathrm{sp}}(f_{\mathrm{cm}})\beta_{RH}\beta_{\mathrm{sp}}(t - t_{\mathrm{pc}}) \tag{14}$$

where $\epsilon_{\mathrm{sp}}(f_{\mathrm{cm}})$, $\beta_{RH}$ are factors depending on the concrete strength and the relative humidity, respectively, which are defined as

$$\epsilon_{\mathrm{sp}}(f_{\mathrm{cm}}) = [160 + \beta_{\mathrm{sc}}(90 - f_{\mathrm{cm}})]10^{-6}, \tag{15a}$$

$$\beta_{RH} = \begin{cases} -1.55(1 - (RH/100)^3), & \text{for } 40\% \le RH \le 99\% \quad \text{(stored in air)} \\ +0.25(1 - (RH/100)^3) & \text{for } RH \ge 99\% \quad \text{(immersed in water)} \end{cases} \tag{15b}$$

where $\beta_{\mathrm{sc}}$ is a coefficient depending on type of cement. Moreover, $\beta_{\mathrm{sp}}(t-t_{\mathrm{pc}})$ in Eq. (14) is a coefficient for the development of shrinkage with time, which is estimated from

$$\beta_{\mathrm{sp}}(t - t_{\mathrm{pc}}) = [(t - t_{\mathrm{pc}})/(0.035h_0^2 + t - t_{\mathrm{pc}})]^{0.5} \tag{16}$$

### 2.4. For each beam

Each beam undergoes transverse deflection and axial deformation. Thus, for the transverse deflection we have

$$E_{\mathrm{b}}I_{\mathrm{b}}\frac{\mathrm{d}^4 w_{\mathrm{b}}}{\mathrm{d}x^4} - N_{\mathrm{b}}\frac{\partial^2 w_{\mathrm{b}}}{\partial x^2} = q_z - \frac{\partial M_{\mathrm{b}}}{\partial x} \quad \text{in } L_k, \quad k = 1, 2, \ldots, K \tag{17}$$

$$a_1 w_{\mathrm{b}} + a_2 V = a_3 \quad \text{at the beam ends } x = 0, l \tag{18a}$$

$$b_1\frac{\partial w_{\mathrm{b}}}{\partial x} + b_2 M = b_3 \tag{18b}$$

where $w_{\mathrm{b}} = w_{\mathrm{b}}(x, t)$ is the time dependent transverse deflection of the beam; $E_{\mathrm{b}}I_{\mathrm{b}}$ is its flexural rigidity; $N_{\mathrm{b}} = N_{\mathrm{b}}(x, t)$ is the axial force at the neutral axis; $V$, $M$ are the reaction and the bending moment at the beam ends, respectively; $a_i$, $b_i$ ($i$ = 1, 2, 3) are coefficients specified at the boundary of the beam. It is apparent that all types of the conventional boundary conditions (clamped, simply supported, free or guided edge) can be derived from Eqs. (18a,b) by specifying appropriately the coefficients $a_i$, $b_i$ (e.g. for a simply supported end it is $a_1 = b_2 = 1$, $a_2 = a_3 = b_1 = b_3 = 0$).

Since the linear beam bending theory is considered, the axial force of the beam does not depend on the deflection $w_{\mathrm{b}}$. The axial deformation of the beam arisen from the in-plane axial force $q_x$ is described by solving independently the boundary value problem, i.e.

$$E_{\mathrm{b}}A_{\mathrm{b}}\frac{\partial^2 u_{\mathrm{b}}}{\partial x^2} = -q_x \quad \text{in } L_k, \quad k = 1, 2, \ldots, K \tag{19}$$

$$c_1 u_{\mathrm{b}} + c_2 N = c_3 \quad \text{at the beam ends } x = 0, l \tag{20}$$

where $N$ is the axial reaction at the beam ends.

Eqs. (1), (11a), (11b), (17), and (19) constitute a set of five coupled partial differential equations

including seven unknowns, namely $w_p$, $u_p$, $v_p$, $w_b$, $u_b$, $q_x$, $q_z$. Two additional equations are required, which result from the continuity conditions of the displacements in the direction of the $z$- and $x$-axes at the interface between the plate and the beams. These conditions can be expressed as

$$w_p = w_b \tag{21}$$

$$u_p - \frac{h_p}{2}\frac{\partial w_p}{\partial x} = u_b + \frac{h_b}{2}\frac{\partial w_b}{\partial x} \tag{22}$$

It must be noted that the coupling of Eqs. (1) and (11a,b), as well as Eqs. (17) and (19) is non-linear due to the terms including the unknown membrane and axial forces, respectively.

## 3. Numerical solution

The numerical solution of the described plate bending, plane stress, beam bending and axial beam problems is achieved using the AEM as this is presented in detail by Sapountzakis and Katsikadelis (1998). The main points of the numerical solution are summarized below.

### 3.1. The Analog Equation Method for the plate equation

Let $w_p$ be the sought solution of the boundary value problem (1), (2a,b). If the biharmonic operator is applied to this function we have

$$\nabla^4 w_p = q_p \quad \text{in } \Omega \tag{23}$$

Eq. (23) indicates that the solution of the original problem, Eq. (1), can be obtained from the solution of a linear plate bending problem with unit stiffness, under the same boundary conditions and subjected to the fictitious load distribution $q_p(\mathbf{x})$. This problem is readily solved if the fictitious loading were known.

Thus, the problem is converted to that of establishing the unknown load density $q_p(\mathbf{x})$. This is accomplished using the Boundary Element Method (BEM) as follows.

The solution of Eq. (23) is given in the integral form as

$$\epsilon w_p(\mathbf{x}) = \int_\Omega w_p^* q_p \, d\Omega - \int_\Gamma \left( w_p^* V_n - \frac{\partial w_p^*}{\partial n} M_n + w_p V_n^* - \frac{\partial w_p}{\partial n} M_n^* \right) ds - \sum_k (w_p^* \| T_n \|_k - w_p \| T_n^* \|_k) \tag{24}$$

where $\epsilon = 1$, $1/2$ or $0$ depending on whether the point $\mathbf{x}$ is inside the domain $\Omega$, on the boundary $\Gamma$, or outside $\Omega$, respectively. The boundary has been assumed smooth at $\mathbf{x} \in \Gamma$. Moreover, $w_p^*$ is the fundamental solution, which is given as

$$w_p^* = \frac{1}{8\pi} r^2 \ln r \tag{25}$$

with $r = [(\xi - x)^2 + (\eta - y)^2]^{1/2}$, $x, y \in \Omega \cup \Gamma$, $\xi, \eta \in \Gamma$. The quantities $M_n^*$ and $V_n^*$ are obtained from Eqs. (3) and (4), respectively, by replacing $w_p$ with $w_p^*$.

Eq. (24) and its normal derivative for $\mathbf{x} \in \Gamma$ yield the following boundary integral equations

$$\frac{1}{2}w_{\mathrm{p}}(\mathbf{x}) = \int_{\Omega} w_{\mathrm{p}}^{*} q_{\mathrm{p}}\,\mathrm{d}\Omega - \int_{\Gamma}\left(w_{\mathrm{p}}^{*}V_{\mathrm{n}} - \frac{\partial w_{p}^{*}}{\partial n}M_{\mathrm{n}} + w_{\mathrm{p}}V_{\mathrm{n}}^{*} - \frac{\partial w_{\mathrm{p}}}{\partial n}M_{\mathrm{n}}^{*}\right)\mathrm{d}s - \sum_{k}(w_{\mathrm{p}}^{*}\|T_{\mathrm{n}}\|_{k} - w_{\mathrm{p}}\|T_{\mathrm{n}}^{*}\|_{k}) \quad (26a)$$

$$\frac{1}{2}\frac{\partial w_{\mathrm{p}}(\mathbf{x})}{\partial n_{x}} = \int_{\Omega}\frac{\partial w_{\mathrm{p}}^{*}}{\partial n_{x}}q_{\mathrm{p}}\,\mathrm{d}\Omega - \int_{\Gamma}\left(\frac{\partial w_{\mathrm{p}}^{*}}{\partial n_{x}}V_{\mathrm{n}} - \frac{\partial^{2}w_{\mathrm{p}}^{*}}{\partial n_{x}\,\partial n}M_{\mathrm{n}} + w_{\mathrm{p}}\frac{\partial}{\partial n_{x}}V_{\mathrm{n}}^{*} - \frac{\partial w_{\mathrm{p}}}{\partial n}\frac{\partial}{\partial n_{x}}M_{\mathrm{n}}^{*}\right)\mathrm{d}s$$
$$- \sum_{k}\left(\frac{\partial w_{\mathrm{p}}^{*}}{\partial n_{x}}\|T_{\mathrm{n}}\|_{k} - w_{\mathrm{p}}\frac{\partial}{\partial n_{x}}\|T_{\mathrm{n}}^{*}\|_{k}\right) \quad (26b)$$

Eqs. (26a,b) together with Eqs. (2a,b) can be employed to express the unknown boundary quantities $w_{\mathrm{p}}$, $\partial w_{\mathrm{p}}/\partial n$, $M_{\mathrm{n}}$, $V_{\mathrm{n}}$ in terms of $q_{\mathrm{p}}$. This is accomplished numerically evaluating the boundary integrals using constant boundary elements and the domain integrals using constant cells. The domain discretization is shown in Fig. 4. If $N$ is the number of boundary nodal points and $M$ that of the domain nodal points, the discretized counterpart of Eq. (24) when applied to all nodal points in $\Omega$ after elimination of the $4N$ boundary quantities yields

$$\{w_{\mathrm{p}}\} = [P]\{q_{\mathrm{p}}\} \quad (27)$$

where $[P]$ is a known $M \times M$ coefficient matrix.

Further, differentiating Eq. (24) for $\mathbf{x} \in \Omega$ we obtain

$$w_{\mathrm{p},\,x}(\mathbf{x}) = \int_{\Omega} w_{\mathrm{p},\,x}^{*} q_{\mathrm{p}}\,\mathrm{d}\Omega - \int_{\Gamma}\left(w_{\mathrm{p},\,x}^{*}V_{\mathrm{n}} - \left(\frac{\partial w_{\mathrm{p}}^{*}}{\partial n}\right)_{,\,x}M_{\mathrm{n}} + w_{\mathrm{p}}(V_{\mathrm{n}}^{*})_{,\,x} - \frac{\partial w_{\mathrm{p}}}{\partial n}(M_{\mathrm{n}}^{*})_{,\,x}\right)\mathrm{d}s$$
$$- \sum_{k}(w_{\mathrm{p},\,x}^{*}\|T_{\mathrm{n}}\|_{k} - w_{\mathrm{p}}\|T_{\mathrm{n},\,x}^{*}\|_{k}) \quad (28a)$$

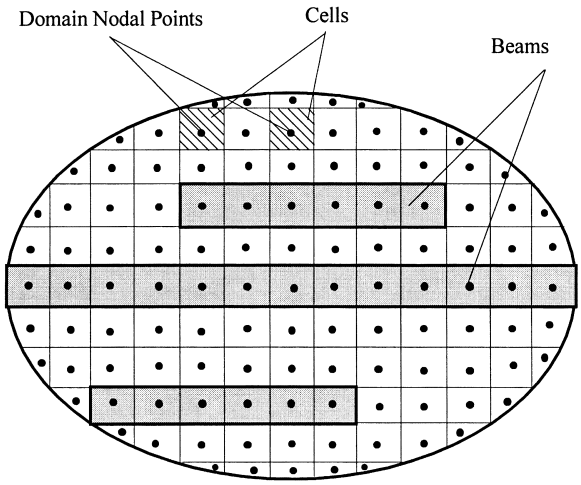


Fig. 4. Discretization of the plate.

$$w_{\mathrm{p},\,xx}(\mathbf{x}) = \int_{\Omega} w^*_{\mathrm{p},\,xx} q_{\mathrm{p}}\,\mathrm{d}\Omega - \int_{\Gamma}\left(w^*_{\mathrm{p},\,xx} V_{\mathrm{n}} - \left(\frac{\partial w^*_{\mathrm{p}}}{\partial n}\right)_{,\,xx} M_{\mathrm{n}} + w_{\mathrm{p}}(V^*_{\mathrm{n}})_{,\,xx} - \frac{\partial w_{\mathrm{p}}}{\partial n}(M^*_{\mathrm{n}})_{,\,xx}\right)\mathrm{d}s$$

$$- \sum_k (w^*_{\mathrm{p},\,xx}\|T_{\mathrm{n}}\|_k - w_{\mathrm{p}}\|T^*_{\mathrm{n},\,xx}\|_k) \tag{28b}$$

$$w_{\mathrm{p},\,yy}(\mathbf{x}) = \int_{\Omega} w^*_{\mathrm{p},\,yy} q_{\mathrm{p}}\,\mathrm{d}\Omega - \int_{\Gamma}\left(w^*_{\mathrm{p},\,yy} V_{\mathrm{n}} - \left(\frac{\partial w^*_{\mathrm{p}}}{\partial n}\right)_{,\,yy} M_{\mathrm{n}} + w_{\mathrm{p}}(V^*_{\mathrm{n}})_{,\,yy} - \frac{\partial w_{\mathrm{p}}}{\partial n}(M^*_{\mathrm{n}})_{,\,yy}\right)\mathrm{d}s$$

$$- \sum_k (w^*_{\mathrm{p},\,yy}\|T_{\mathrm{n}}\|_k - w_{\mathrm{p}}\|T^*_{\mathrm{n},\,yy}\|_k) \tag{28c}$$

$$w_{\mathrm{p},\,xy}(\mathbf{x}) = \int_{\Omega} w^*_{\mathrm{p},\,xy} q_{\mathrm{p}}\,\mathrm{d}\Omega - \int_{\Gamma}\left(w^*_{\mathrm{p},\,xy} V_{\mathrm{n}} - \left(\frac{\partial w^*_{\mathrm{p}}}{\partial n}\right)_{,\,xy} M_{\mathrm{n}} + w_{\mathrm{p}}(V^*_{\mathrm{n}})_{,\,xy} - \frac{\partial w_{\mathrm{p}}}{\partial n}(M^*_{\mathrm{n}})_{,\,xy}\right)\mathrm{d}s$$

$$- \sum_k (w^*_{\mathrm{p},\,xy}\|T_{\mathrm{n}}\|_k - w_{\mathrm{p}}\|T^*_{\mathrm{n},\,xy}\|_k) \tag{28d}$$

Using the same boundary and domain discretization and once more eliminating the boundary quantities we obtain

$$\{w_{\mathrm{p},\,x}\} = [P_x]\{q_{\mathrm{p}}\} \tag{29a}$$

$$\{w_{\mathrm{p},\,xx}\} = [P_{xx}]\{q_{\mathrm{p}}\} \tag{29b}$$

$$\{w_{\mathrm{p},\,yy}\} = [P_{yy}]\{q_{\mathrm{p}}\} \tag{29c}$$

$$\{w_{\mathrm{p},\,xy}\} = [P_{xy}]\{q_{\mathrm{p}}\} \tag{29d}$$

where $[P_x]$, $[P_{xx}]$, $[P_{yy}]$, $[P_{xy}]$ are known $M \times M$ coefficient matrices. Note that Eqs. (27) and (29a,b,c,d) are valid for homogeneous boundary conditions ($\alpha_3 = \beta_3 = 0$). For non-homogeneous boundary conditions, an additive constant vector will appear on the right-hand-side of these equations.

The final step of AEM is to apply Eq. (1) to the $M$ nodal points inside $\Omega$. This yields

$$D\{q_{\mathrm{p}}\} - ([N_x][P_{xx}] + 2[N_{xy}][P_{xy}] + [N_y][P_{yy}])\{q_{\mathrm{p}}\} = \{g\} - [Z]\{q_z\} - [X]\{q_x\} \tag{30}$$

where $[N_x]$, $[N_{xy}]$ and $[N_y]$ are unknown diagonal $M \times M$ matrices including the values of the in-plane forces; $\{q_z\}$ and $\{q_x\}$ are vectors with $L$ elements; $L$ is the total number of the nodal points at the interfaces; $[Z]$ is a position vector which converts the vector $\{q_z\}$ into a vector with length $M$. The matrix $[X]$ results after approximating the derivative of $M_{\mathrm{p}}$ with finite differences. Its dimensions are also $M \times L$.

### 3.2. The Analog Equation Method for the plane stress problem

The AEM for this problem is presented in Katsikadelis and Kandilas (1994). Following this procedure and using the same boundary and domain discretization the membrane forces for homogeneous

boundary conditions (12a,b) ($\gamma_3 = \delta_3 = 0$) are expressed as follows

$$\{N_x\} = [F_x]\{q_x\} \tag{31a}$$

$$\{N_{xy}\} = [F_{xy}]\{q_x\} \tag{31b}$$

$$\{N_y\} = [F_y]\{q_x\} \tag{31c}$$

where $[F_x]$, $[F_{xy}]$ and $[F_y]$ are known matrices with dimensions $M \times L$.

### 3.3. The Analog Equation Method for the deflection of the beams

Similarly with the plate, let $w_b$ be the sought solution of the boundary value problem described by Eqs. (17) and (18a,b). Differentiating this function four times yields

$$\frac{d^4 w_b}{dx^4} = q_b \tag{32}$$

Eq. (32) indicates that the solution of the original problem can be obtained as the deflection of a beam with unit flexural rigidity subjected only to a transverse fictitious load $q_b$ under the same boundary conditions. The fictitious load is unknown. However, it can be established using the BEM as follows.

The solution of Eq. (32) is given in integral form as

$$w_b(x) = \int_0^l w_b^* q_p \, ds + \left[ w_b^* V - \frac{\partial w_b^*}{\partial x} M + w_b V^* - \frac{\partial w_b}{\partial x} M^* \right]_0^l \tag{33}$$

where $w_b^*$ is the fundamental solution which is given as

$$w_b^* = \tfrac{1}{12} l^3 (2 + |\rho|^3 - 3|\rho|^2) \tag{34}$$

with $\rho = r/l$, $r = \xi - x$, $x \in L_k$, $k = 1, 2, \ldots, K$, $\xi$ at the beam ends $x = 0, l$ and the quantities $M^*$ and $V^*$ are given as

$$M^* = \tfrac{1}{2} l (1 - |\rho|) \tag{35a}$$

$$V^* = -\tfrac{1}{2} \operatorname{sgn} \rho \tag{35b}$$

Further, differentiating Eq. (33) for $x \in L_k$, $k = 1, 2, \ldots, K$ we obtain

$$w_{b,\,x}(x) = \int_0^l w_{b,\,x}^* q_b \, ds - \left[ w_{b,\,x}^* V - \left( \frac{\partial w_b^*}{\partial x} \right)_{,\,x} M + w_b (V^*)_{,\,x} - \frac{\partial w_b}{\partial x} (M^*)_{,\,x} \right]_0^l \tag{36a}$$

$$w_{b,\,xx}(x) = \int_0^l w_{b,\,xx}^* q_b \, ds - \left[ w_{b,\,xx}^* V - \left( \frac{\partial w_b^*}{\partial x} \right)_{,\,xx} M + w_b (V^*)_{,\,xx} - \frac{\partial w_b}{\partial x} (M^*)_{,\,xx} \right]_0^l \tag{36b}$$

Eqs. (33) and (36a) for $x = 0$ and $x = l$ together with Eqs. (18a,b) can be employed to express the unknown boundary quantities $w_b$, $\partial w_b / \partial n$, $M$, $V$ in terms of $q_b$. Moreover, the discretized counterpart of

Eqs. (33) and (36a,b) when applied to the $L$ nodal points at the interfaces after elimination of the boundary quantities yields

$$\{w_{\mathrm{b}}\} = [B]\{q_{\mathrm{b}}\} \tag{37a}$$

$$\{w_{\mathrm{b},\,x}\} = [B_x]\{q_{\mathrm{b}}\} \tag{37b}$$

$$\{w_{\mathrm{b},\,xx}\} = [B_{xx}]\{q_{\mathrm{b}}\} \tag{37c}$$

where $[B]$, $[B_x]$, $[B_{xx}]$ are known $L \times L$ coefficient matrices. Note that Eqs. (37a,b,c) are valid for homogeneous boundary conditions ($a_3 = b_3 = 0$). For non-homogeneous boundary conditions, an additive constant vector will appear on the right-hand-side of these equations.

The final step of AEM is to apply Eq. (8) to the $L$ nodal points at the interfaces. This yields

$$E_{\mathrm{b}} I_{\mathrm{b}}\{q_{\mathrm{b}}\} - [N_{\mathrm{b}}][B_{xx}]\{q_{\mathrm{b}}\} = \{q_z\} - [Q]\{q_x\} \tag{38}$$

where $[N_{\mathrm{b}}]$ is an unknown diagonal $L \times L$ matrix including the values of the in-plane forces; $\{q_z\}$ and $\{q_x\}$ are vectors with $L$ elements. The matrix $[Q]$ results after approximating the derivative of $M_{\mathrm{b}}$ with finite differences. Its dimensions are also $L \times L$.

### 3.4. The Analog Equation Method for the axial deformation of the beams

The solution of Eq. (19) is given in integral form as

$$u_{\mathrm{b}}(x) = -\int_0^l u_{\mathrm{b}}^* q_x \, \mathrm{d}s + \left[ u_{\mathrm{b}}^* \frac{\mathrm{d}u_{\mathrm{b}}}{\mathrm{d}x} - \frac{\mathrm{d}u_{\mathrm{b}}^*}{\mathrm{d}x} u_{\mathrm{b}} \right]_0^l \tag{39}$$

where

$$u_{\mathrm{b}}^* = \frac{1}{2E_{\mathrm{b}}A_{\mathrm{b}}}(l - |\, r\,|) \tag{40}$$

Following the same procedure as in Section 3.3 the axial force at the neutral axis of the beam for homogeneous boundary conditions (20) ($c_3 = 0$) can be expressed as follows

$$\{N_{\mathrm{b}}\} = [F_{\mathrm{b}}]\{q_x\} \tag{41}$$

where $[F_{\mathrm{b}}]$ is a known matrix with dimensions $L \times L$.

Eqs. (30) and (38) after elimination of the quantities $N_x$, $N_y$, $N_{xy}$, $N_{\mathrm{b}}$ using Eqs. (31a,b,c), and (41) together with continuity conditions (21), and (22), which after discretization at the $L$ nodal points at the interfaces are written as

$$\{w_{\mathrm{p}}\} = \{w_{\mathrm{b}}\} \tag{42a}$$

$$\{u_{\mathrm{p}}\} - \frac{h_{\mathrm{p}}}{2}\{w_{\mathrm{p},\,x}\} = \{u_{\mathrm{b}}\} + \frac{h_{\mathrm{b}}}{2}\{w_{\mathrm{b},\,x}\} \tag{42b}$$

constitute a non-linear system of equations with respect to $q_z$, $q_x$, $q_{\mathrm{p}}$, $q_{\mathrm{b}}$. This system is solved using iterative numerical methods. Subsequently, the deflection at any interior point $\mathbf{x} \in \Omega$ of the stiffened plate is established using the discretized counterpart of Eq. (24) when applied to this point.

For the solution of the non-linear system of equations the two-term acceleration method (Isaacson and Keller, 1966; Sapountzakis and Katsikadelis, 1992) has been employed. According to this method, an initial vector, say $\boldsymbol{q}_x^{(0)}=\mathbf{0}$ is assumed. Using this vector and Eqs. (38) and (42a,b) the values of the vectors $\boldsymbol{q}_z^{(0)}$, $\boldsymbol{q}_{\mathrm{p}}^{(0)}$, $\boldsymbol{q}_{\mathrm{b}}^{(0)}$ are computed. Introducing these values into Eq. (30) a vector $\boldsymbol{q}_x^{(1')}$ is obtained. To accelerate convergence the new initial vector is given as

$$q_x^{(1)} = \alpha q_x^{(0)} + \beta q_x^{(1')} \tag{43}$$

where $\alpha$, $\beta$ are appropriately chosen weight factors with $\alpha+\beta=1$.

## 4. Numerical examples

On the basis of the analytical and numerical procedures presented in the previous sections, a computer program has been written and representative examples have been studied to demonstrate the efficiency and the range of applications of the developed model. In all the examples treated, the numerical results have been obtained using 54 constant boundary elements and 162 constant domain rectangular cells. For these examples 350 iterations were required to achieve a tolerance limit of 1.0E−03.

### 4.1. Example 1

A rectangular plate with dimensions $a \times b = 18.0 \times 9.0$ m subjected to a uniform load $g = 10$ kN/m$^2$ and stiffened by an I-section beam (Fig. 5) through the centre line of the plate has been studied. The plate is simply supported along its small edges, while the other two edges are free according to the transverse boundary conditions and $u_x=u_y=0$ along the edges $x=a_{\mathrm{p}}/2$, $x=-a_{\mathrm{p}}/2$, $N_y=N_{xy}=0$ along the edges $y=b_{\mathrm{p}}/2$, $y=-b_{\mathrm{p}}/2$ according to the in-plane boundary conditions. The numerical results have been obtained for different values of the height $h_{\mathrm{web}}$ of the beam. In Table 1 the deflections of the stiffened plate at its centre and at the middle of the free edge are shown as compared with those obtained from a FEM solution (Sofistik, 1995), which cannot include the in-plane forces and deformations. The discrepancy of the results, which is more pronounced at the centre of the plate, is

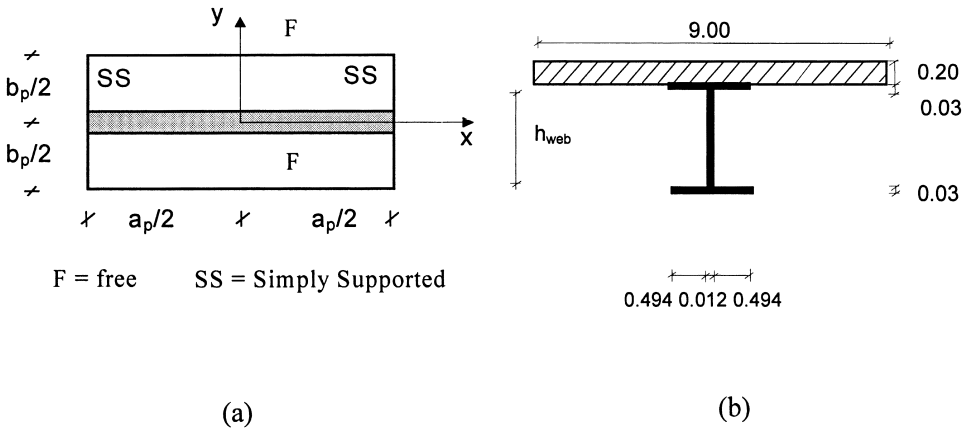


Fig. 5. Plan (a) and cross section (b) of the stiffened plate of Example 1.

Table 1
Deflections $w$ (m) at the centre and at the middle of the free edge of the stiffened plate of Example 1 ($E_p = 3.0 \times 10^7$ kN/m$^2$, $h_p = 0.20$ m, $\nu = 0.154$)

| $h_{web}$ | Centre | | Middle of the free edge | |
|---|---|---|---|---|
| | AEM | FEM (Sofistik, 1995) | AEM | FEM (Sofistik, 1995) |
| 2.00 | 0.0008 | 0.0239 | 0.0206 | 0.0453 |
| 1.50 | 0.0013 | 0.0369 | 0.0212 | 0.0583 |
| 1.00 | 0.0029 | 0.0596 | 0.0227 | 0.0809 |
| 0.50 | 0.0090 | 0.1012 | 0.0287 | 0.1226 |
| No beam | 0.6719 | 0.6721 | 0.6938 | 0.6944 |

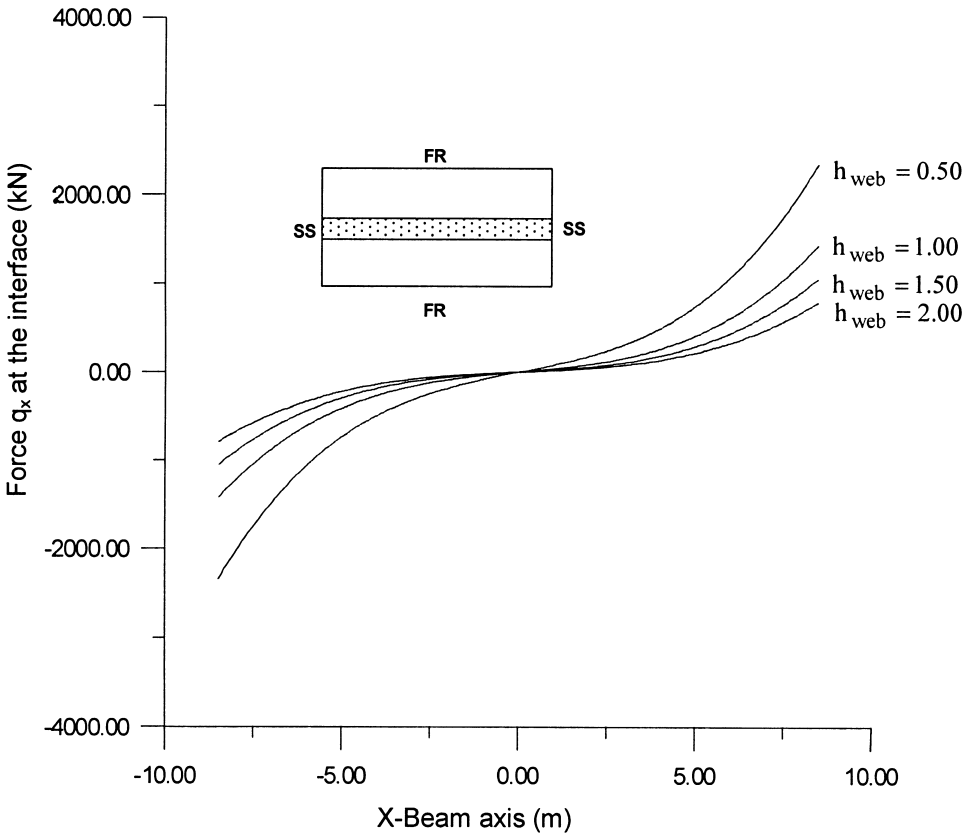


Fig. 6. Distribution of the $q_x$ forces along the beam axis of the stiffened plate of Example 1.

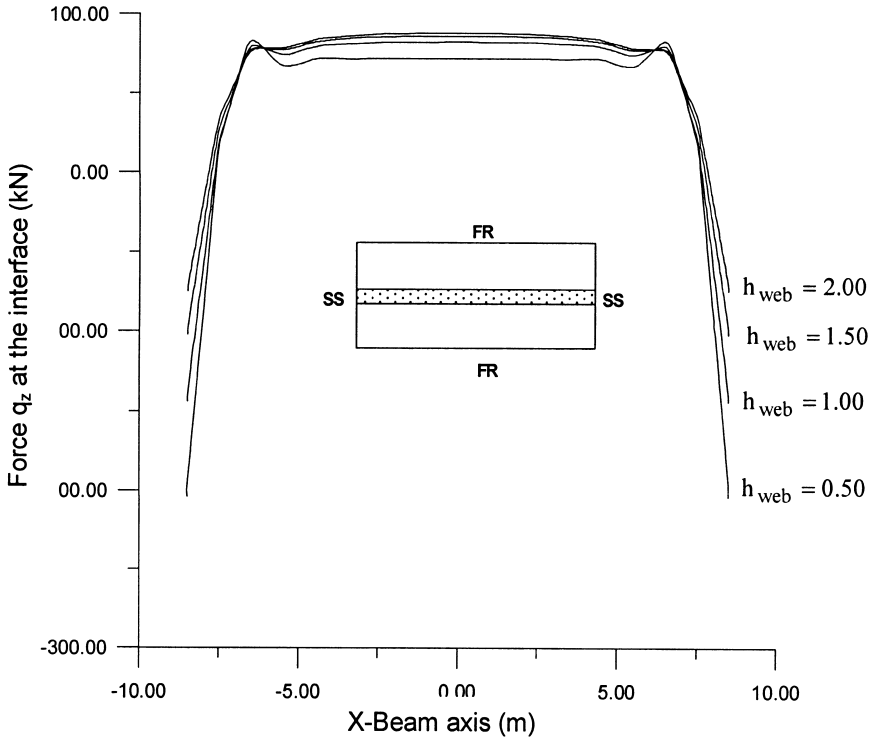


Fig. 7. Distribution of the $q_z$ forces along the beam axis of the stiffened plate of Example 1.

obvious. Moreover, in Figs. 6 and 7 the distributions of the interface forces $q_x$ and $q_z$ are presented for various values of the height $h_{\text{web}}$ of the beam.

### 4.2. Example 2

Creep and shrinkage effect on the stiffened plate of Example 1 has been studied. The following data have been used for the numerical results: concrete C25/30, $f_{\text{cm}} = 25$ N/mm$^2$, $RH = 40\%$, $t_{\text{p}} = 28$ days, $E_{\text{pl}} = E_{\text{c28}} = 32.55$ kN/mm$^2$, $h_{\text{p}} = 0.20$ m, $\nu = 0.154$, $\beta_{\text{sc}} = 5$ (normal or rapid hardening cement), $a =$

Table 2
Deflections $w$ (m) at the centre of the stiffened plate of Example 2

| Age of concrete $t$ (days) | $h_{\text{web}}$ of the stiffening beam | | | | | |
|---|---|---|---|---|---|---|
| | 1.00 | | 1.50 | | 2.00 | |
| | AEM | FEM (Sofistik, 1995) | AEM | FEM (Sofistik, 1995) | AEM | FEM (Sofistik, 1995) |
| 30 | 0.2913E−2 | 0.6175E−1 | 0.1363E−2 | 0.3773E−1 | 0.7692E−3 | 0.2427E−1 |
| 100 | 0.3049E−2 | 0.6399E−1 | 0.1430E−2 | 0.3869E−1 | 0.8093E−3 | 0.2472E−1 |
| 150 | 0.3071E−2 | 0.6516E−1 | 0.1442E−2 | 0.3915E−1 | 0.8162E−3 | 0.2491E−1 |
| 300 | 0.3097E−2 | 0.6568E−1 | 0.1456E−2 | 0.3935E−1 | 0.8251E−3 | 0.2498E−1 |
| 1000 | 0.3111E−2 | 0.6618E−1 | 0.1465E−2 | 0.3948E−1 | 0.8318E−3 | 0.2499E−1 |

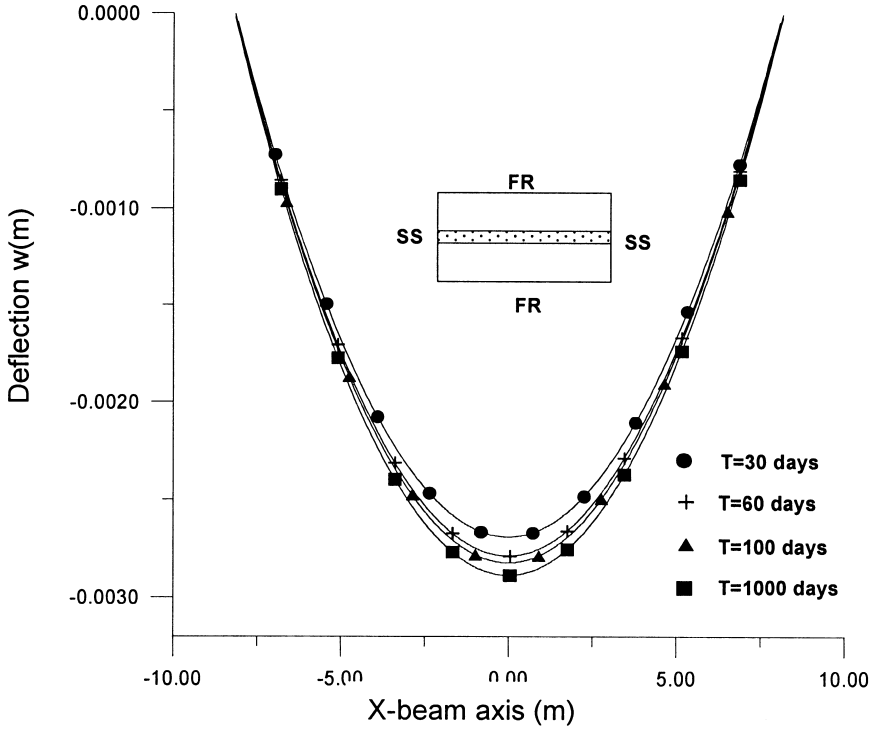


Fig. 8. Deflections along the beam axis with $h_{web} = 1.00$ m of the stiffened plate of Example 2.

$10^{-5\circ}$C. In Fig. 8 the distributions of the deflection $w$ along the beam axis for the height of the beam $h_{web} = 1.00$ m and for various instants are shown. From this figure the predominant action of creep compared to shrinkage at all times is obvious. Moreover, in Table 2 the deflections $w$ at the centre of the stiffened plate for different values of the height $h_{web}$ and for various instants are shown as compared with those obtained from a FEM solution (Sofistik, 1995), which cannot include the in-plane forces and deformations. The discrepancy of the results is once more obvious. According to the obtained interface

Table 3
Time development of the interface forces $q_x$ at point $x = 8.5$ of the interface of the stiffened plate of Example 2

| Age of concrete $t$ (days) | $h_{web}$ of the stiffening beam | | | |
|---|---|---|---|---|
| | 0.50 | 1.00 | 1.50 | 2.00 |
| 30 | 2564 | 1621 | 1177 | 920 |
| 60 | 2553 | 1618 | 1175 | 919 |
| 100 | 2542 | 1613 | 1171 | 916 |
| 150 | 2532 | 1607 | 1167 | 913 |
| 200 | 2523 | 1603 | 1164 | 911 |
| 300 | 2510 | 1596 | 1159 | 907 |
| 500 | 2493 | 1586 | 1152 | 901 |
| 1000 | 2468 | 1572 | 1142 | 894 |

forces $q_x$ of the stiffened plate, in Table 3 the time development of these forces at point $x = 8.5$ m of the interface for different values of the height $h_{\text{web}}$ of the beam is presented.

## 5. Concluding remarks

A solution to the bending problem of reinforced concrete slabs stiffened by steel beams including creep and shrinkage effect is presented. A realistic model has been adopted, which contrary to other approaches, takes into account the in-plane forces and deformations of the plate as well as the axial forces and deformations of the beams. The main conclusions that can be drawn from this investigation are:

1. The evaluated lateral deflections of the plate–beams system are found to exhibit considerable discrepancy from those of other models, which neglect in-plane and axial forces and deformations.
2. The adopted model permits the evaluation of the in-plane shear forces at the interface between the plate and the beams, the knowledge of which is very important in the design of composite steel–concrete structures (estimation of shear connectors).
3. The proposed model permits the study of the behaviour of a composite steel–concrete stiffened plate due to the opposed effects of creep and shrinkage. In the studied examples the predominant action of creep compared to shrinkage at all times was verified.
4. The effect of creep and shrinkage is more pronounced in the case of low height beams and in the early age of concrete.

## References

Cheung, M.S., Akhras, G., Li, W., 1994. Combined boundary element/finite strip analysis of bridges. Journal of Structural Engineering 120, 716–727.

Eurocode No. 2, 1991. Design of concrete structures, Part 1: general rules and rules for buildings. Eurocode 2 Editorial Group.

Hu, C., Hartley, G.A., 1994. Elastic analysis of thin plates with beam supports. Engineering Analysis with Boundary Elements 13, 229–238.

Isaacson, E., Keller, H., 1966. Analysis of Numerical Methods. John Wiley and Sons, New York.

Katsikadelis, J.T. 1994. The analog equation method — a powerful BEM-based solution technique for solving linear and non-linear engineering problems. In: Boundary Element Method XVI. Computational Mechanics Publications, pp. 167–182.

Katsikadelis, J.T., Kandilas, C.B., 1994. Solving the elastostatic problem by the analog equation method. Advances in Computational Mechanics, pp. 178–269.

King, I.P., Zienkienwicz, O.C., 1968. Slab bridges with arbitrary shape and support conditions: a general method of analysis based on finite element method. Proceedings of the Institution of Civil Engineers 40, 9–36.

Kukreti, A.R., Cheraghi, E., 1993. Analysis procedure for stiffened plate systems using an energy approach. Computers and Structures 46, 649–657 4 February.

Kukreti, A.R., Rajapaksa, Y., 1990. Analysis procedure for ribbed and grid plate systems used for bridge decks. Journal of Structural Engineering, ASCE 116, 372–391 2 February.

Nerantzaki, M.S. 1994. Solving plate bending problems by the analog equation method. In: Boundary Element Method XVI. Computational Mechanics Publications, pp. 283–291.

Ng, S.F., Cheung, M.S., Xu, T., 1990. A combined boundary element and finite element solution of slab and slab-on-girder bridges. Computers and Structures 37, 1069–1075.

de Paiva, J.B., 1996. Boundary element formulation of building slabs. Engineering Analysis with Boundary Elements 17, 105–110.

Pama, R.P., Cusens, A.R., 1967. Edge beam stiffening of multibeam bridges. Journal of the Structural Division, ASCE 93, 141–161 ST2 April.

Powell, G.H., Ogden, D.W., 1969. Analysis of orthotropic steel plate bridge decks. Journal of the Structural Division, ASCE 95, 909–921 ST5 May.

Sapountzakis, E.J., Katsikadelis, J.T., 1992. Unilaterally supported plates on elastic foundations by the boundary element method. Journal of Applied Mechanics, ASME 59, 580–586.

Sapountzakis, E.J., Katsikadelis, J.T. 1998. Analysis of plates reinforced with beams. In: Proceedings of the 5th National Congress of H.S.T.A.M., Ioannina 27–30 August.

Sofistik, GmbH, 1995. Software für Statik und Konstruktion Gesellschaft mit beschränkter Haftung. Ringstr. 29a, D-8042, Oberschleißheim.

Tanaka, M., Bercin, A.N. 1997. A boundary element method applied to the elastic bending problem of stiffened plates. In: Boundary Element Method XIX. Computational Mechanics Publications, pp. 203–212.

Trost, H., Wolff, J., 1970. Zur Wirklichkeitsnahen Ermittlung der Beanspruchungen in Abschnittsweise Hergestellten Spannbetontragwerken. Der Bauingenieur 45, 155–169.